Supporting Information

Controlling electrocatalytic nitrate reduction efficiency by utilizing dπ-pπ interactions in parallel stacking molecular systems

Sourav Bhowmick[a,d], Ashadul Adalder[a], Abhishek Maiti[b,¥], Samadhan Kapse[c], Ranjit Thapa[c], Supriya Mondal[d] and Uttam Kumar Ghorai[a]*

[1]Department of Industrial Chemistry & Applied Chemistry, Swami Vivekananda Research Centre, Ramakrishna Mission Vidyamandira, Belur Math, Howrah - 711202, India

[2]School of Physical Sciences, Indian Association for the Cultivation of Science, Jadavpur, Kolkata, 700032 India

[3]Department of Physics and Centre for Computational and Integrative Sciences, SRM University – AP, Amaravati 522240, Andhra Pradesh, India

[4]Department of Physics, Government General Degree College Chapra, Nadia, West Bengal, 741123, India

[¥]Present address, Laboratoire de Physique des Solides, Universite Paris-Saclay, CNRS, Orsay, 91405, France

* E-mail: uttam.indchem@vidyamandira.ac.in

Experimental Section:

Materials: Copper (II) acetate monohydrate (Merck), phthalonitrile (Sigma Aldrich), ammonium heptamolybdate tetrahydrate (Merck), sodium nitrate (Merck), sodium sulphate (Merck), ammonium sulphate (Merck), ethylene glycol, sodium nitrate–^{15}N (≥98 atom % ^{15}N, Sigma–Aldrich), trisodium citrate dihydrate (Merck), sodium hydroxide (Merck), salicylic acid (Merck), sodium hypochlorite (Merck), sodium nitroprusside dihydrate (Loba Chemie Pvt. Ltd.), para-dimethyl aminobenzaldehyde (Loba Chemie Pvt. Ltd.), *N*-(1-naphthyl)-ethylenediamine dihydrochloride (Loba Chemie Pvt. Ltd.), sulfanilic acid (Loba Chemie Pvt. Ltd.), and acetic acid (Merck) were purchased from the market and used as reagents without further purification. Toray Carbon Paper was purchased from Thermo Scientific. Chemicals were used for electrochemical measurements.

Synthesis of α-CuPc: α-CuPc was synthesised using solvothermal technique. 0.738 g (5.76 mmol) of phthalonitrile, 0.2874 g (1.44 mmol) of copper acetate monohydrate and 20 mg of ammonium heptamolybdate were weighted on a four-digit balance separately and put into a 100-ml beaker, where 48 ml of ethylene glycol was added as a solvent. Then the mixture was heated at ~65 °C with continuous stirring with the help of a magnetic stirrer for 10 minutes. After that, the hot mixture was transferred to a Teflon-lined autoclave. The autoclave was put in an oven for heating at 90^{o}C for 16 hours. After cooling the autoclave to room temperature, the mixture was filtered to get the precipitate and washed thoroughly with ethanol, water and hot 0.1 N HCl to remove impurities. The precipitate was dried at 65^{o}C for 12 hours to get α-CuPc.

Synthesis of β-CuPc: To synthesis of β-CuPc, same conditions were maintained as for synthesis of α-CuPc with some modification. The same moles of phthalonitrile, copper acetate monohydrate and ammonium heptamolybdate were taken in a beaker of 48 ml of ethylene glycol. The mixture was heated at ~65 °C with continuous stirring for 30 minutes. Then the mixture was put in an oven at 180 °C in a Teflon-lined autoclave for 24 hours. After that, the product was collected in the same way as α-CuPc.

Characterizations technique: Phase identification and crystal structures of both types of CuPc were confirmed by X-ray diffraction technique (XRD) using the Bruker D-8 advanced Eco X-ray powder diffractometer at Cu K_{α} (λ = 0.154 nm) monochromatic wavelength, where voltage and current in the system were 40 kV and 25 mA, respectively. The chemical compositions of α-CuPc and β-CuPc were confirmed by X-ray photoelectron spectroscopy with OMICRON-0571. Different types of bonding between the constituent elements of both types of CuPc were studied by the Shimadzu IRAffinity-1S FTIR spectrometer. All

electrochemical experiments were performed in CHI760E workstation. Quantification of ammonia was made using Shimadzu UV-3600 Plus UV-vis spectrophotometer & Eco IC Metrohm (Ion Chromatography). Agilent 8860 GC system was used for gas detection. The morphology of the catalysts was studied by a high-resolution transmission electron microscope (FEG-TEM, JEOL-JEM 2100F).

Electrochemical experiments: All of the electrochemical measurements were performed by a CHI 760E electrochemical setup with a three-electrode system. Catalysts supported on carbon papers were used as working electrode and platinum foil was used as a counter electrode, while a standard potassium chloride-saturated Ag/AgCl electrode was used as a reference electrode. All potentials referenced to the standard potassium chloride-saturated Ag/AgCl electrode were converted to the reversible hydrogen electrode (RHE). Entire electrochemical reactions were done in an H-type cell, where cathode and anode were separated by a chemically treated Nafion 117 membrane. A solution of 0.25 (M) $NaNO_3$ and 0.1(M) Na_2SO_4 was used as electrolyte. Nafion membrane was pre-treated with 5% H_2O_2, 0.05 (M) H_2SO_4 solution and ultra-pure water (resistivity 18.2 MΩ.cm).

Working electrode preparation: 0.8 mg of each freshly synthesised catalyst were weighted on a four-digit balance and taken in two separate vials. 200 µL of isopropanol was added to each vial and sonicated for a few minutes. Then 20 µL of Nafion 117 (5% wt) was added to each vial. Finally, the mixtures were shaken well in a vortex machine to make homogeneous solutions individually. Then 40 µL of each mixture was finely coated on two different 1x1cm^2 carbon paper (0.145 mg/cm^2) and dried well. Thus, catalyst-coated carbon papers were used for electrochemical studies.

Determination of ammonia yield rate and Faradaic efficiency by UV-vis method: Quantification of ammonia, a product of electrocatalysis, was done by the indophenol blue method (**Fig. S6**). In brief, 2 mL of colouring solution containing 5 wt% trisodium citrate dihydrate, 1M sodium hydroxide and 5 wt% salicylic acid, 1 mL of 0.05 M sodium hypochlorite solution as an oxidising agent, and 0.2 mL of (3.34 mmol) sodium nitroprusside dihydrate solution as a catalyst were added to the 2 ml of 100 times diluted electrolyte solution. After 2 hours of incubation in the dark, samples were measured spectrochemically using a UV-vis spectrophotometer, which shows maximum absorbance at 655 nm. For calibration, standard solutions prepared from NH_4SO_4 ranging in concentration from 0.0 µg mL^{-1} to 2.0 µg mL^{-1} were utilised (**Fig. S6a**). The standard calibration curve (y = 0.2511x +0.0128) was obtained from the abs. vs. concentration curve of the standard ammonia solution (**Fig. S6b**). Using this equation, the values of unknown samples were obtained. The

yield rate and Faradaic efficiency (FE) of electrochemical nitrate reduction to ammonia were calculated using the equations mentioned below.

$$\text{Ammonia yield rate} = \frac{\left(C_{NH_3} \text{ x } V\right)}{\left(m_{cat} \text{ x } t\right)}$$

$$FE_{NH_3}\ (\%) = \frac{\left(8 \text{ x } F \text{ x } C_{NH_3} \text{ x } V\right)}{\left(M_{NH_3} \text{ x } Q\right)} \text{ x } 100\%$$

$$FE_{NO_2^-}\ (\%) = \frac{\left(2 \text{ x } F \text{ x } C_{NO_2^-} \text{ x } V\right)}{\left(M_{NO_2^-} \text{ x } Q\right)} \text{ x } 100\%$$

C refers to the concentration of ammonia/nitrite produced after electrolysis. V stands for the total volume used for the electrolyte used in the cathode. m_{cat} stands for mass of catalyst. Here, F is the Faraday constant (96500 C mol^{-1}), M refers to the molecular mass of ammonia/nitrite and Q is the total charge passed through the catalyst surface.

Ammonium ion detection by Ion Chromatography: The ammonia yield formation was further verified by the ion chromatography technique (**Fig. S8**) using Eco IC Metrohm. Metrosep C 6 - 150/4.0 was used as a cationic separation with a flow rate of 0.9 mL/min. 1.7 mmol/L of nitric acid solution was used as eluent. The retention time for peak ammonium ions was ~5.1 min with a pressure of 7.55 MPa.

The standard curve of calibration for ammonium ion detection was used using ammonium sulphate with concentrations ranging from 0.0 µg mL^{-1} to 2.0 µg mL^{-1}(**Fig. S8a**). The concentration of ammonium ions was obtained from the equation y = 0.11427x + 0.00224, obtained from the calibration curve. (**Fig. S8b**)

Hydrazine detection: Spectrophotometrically, hydrazine was detected using Watt and Chrisp method (**Fig. S9**).[1] 2g of para-dimethylaminobenzaldehyde and 10 mL of conc. HCl were dissolved in a 100 mL ethanol solution for making colouring agents. Then 4 mL of colouring agent is mixed with 1 mL of electrolyte, and the mixtures are incubated for 15 minutes. The coloured solutions were measured with UV-vis spectrophotometer at a maximum wavelength of 455 nm.

A standard calibration curve was made from an 80% hydrazine hydrate solution with a standard solution ranging from 0.0 µg mL^{-1} to 1.0 µg mL^{-1} with the same colouring agent treatment as the sample (**Fig. S9a**). The equation found from the calibration curve of absorbance vs. concentration y = 0.28x +0.01367 with R^2 = 0.999 (**Fig. S9b**).

Nitrite ion detection: The concentration of nitrite was detected using UV-vis spectroscopic analysis (**Fig. S10**). A colour solution was prepared by mixing 0.5 g of sulfanilic acid, 5 mg of *N*-(1-naphthyl)-ethylenediamine dihydrochloride, and 5 mL of acetic acid (Merck). Triple-distilled water (Millipore) was added to the mixture with a volume of 100 mL. The colour solution (4 mL) was then added to 1 mL 50 times diluted of electrolyte solution after electrocatalytic reaction, and the mixture was left in the dark for 15 minutes. Then, using a UV-Vis spectrophotometer, the spectrum was captured. The concentration was determined by comparing the absorbance value with a standard calibration curve prepared using a standard 0.0–10 μg mL^{-1} of nitrite concentration. ($y = 0.19443x + 0.19051$, $R^2 = 0.999$) (**Fig. S10b)**

Detection of isotopic levelled ammonium derived from isotopic $NaNO_3$ (^{15}N) by ^1H–NMR:

Isotopically levelled $NaNO_3$ (^{15}N) was used to confirm the source of nitrogen in ammonia. An isotopically levelled $NaNO_3$ (^{15}N) solution was used for electrolysis at –1.1 V vs. RHE for 1 hours and distilled. The ammonia was detected by ^1H-NMR (Bruker 600 MHz, USA) with an internal solution of D_2O (Sigma-Aldrich). The electrolyte solution was made acidic with a 0.05 M H_2SO_4 solution prior to the experiment. A mixture of 0.1 mL of D_2O and 0.4 mL of acidic ammonium solution was used for ^1H-NMR analysis.

Computational details: Density functional theory (DFT) implemented in the Vienna Ab initio Simulation Package (VASP) is used for theoretical computations[2]. Within the Generalized Gradient Approximation (GGA), the Perdew Burke-Ernzerhof (PBE) exchange-correlation functional is employed[3] . For the plane-wave basis set, the projector-augmented wave (PAW) pseudopotential[4] is used, with a cutoff energy of 450 eV. The ionic relaxation loop and electronic self-consistent loop have energy convergence conditions of 10^{-3} eV and 10^{-6} eV, respectively. For the CuPc phthalocyanine system, the gamma point is where the Brillouin zone is sampled. A 15 Å vacuum is provided to reduce interactions between successive images.

The free energy profile is useful method to estimate thermodynamic overpotential (at U=0V, energy of highest uphill step), which is a measure of reaction activity of catalyst. To plot the free energy profile, we need the Gibbs free energies for each reaction step. So, the Gibbs free energies (G) are calculated using the equation $G = E + ZPE – TS - neU$, where E represents the DFT-calculated energy, n is the number of electrons, and U is the applied potential at the electrode [5]. The free energy contributions from zero-point energy (ZPE) and entropy term (TS) are determined by employing density functional theory (DFT) calculations on the vibrational frequencies of adsorbate molecules. This is achieved by fixing the adsorbent

during the calculations. The ZPE correction is calculated as ZPE = ½∑iħωi, where ħ is the reduced Planck's constant and ωiis the frequency of the ith vibrational mode of the adsorbate molecule. The entropic term of the free energy is calculated as:

$$TS_{vib} = k_B T \sum_i [\frac{\hbar\omega_i,}{k_B T\ (e^{\hbar\omega_i/k_B T})} - \ln(1 - e^{-\hbar\omega_i/k_B T})]$$

The DFT energy (E), ZPE, TS and Gibbs free energy (G) values for the free molecules and each intermediates adsorbed on β-CuPc are provided in the **Table S2** of supporting information.

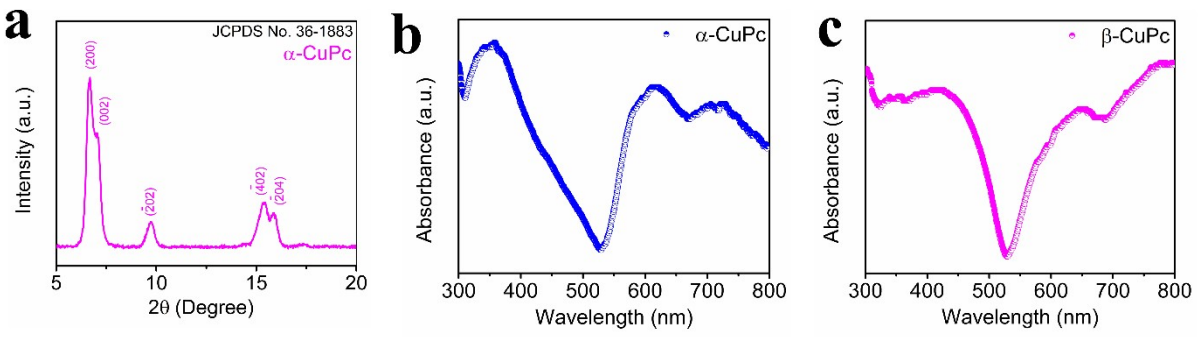

Fig. S1 (a) XRD pattern of α-CuPc **(b-c)** UV- visible Spectra of α-CuPc and β-CuPc respectively.

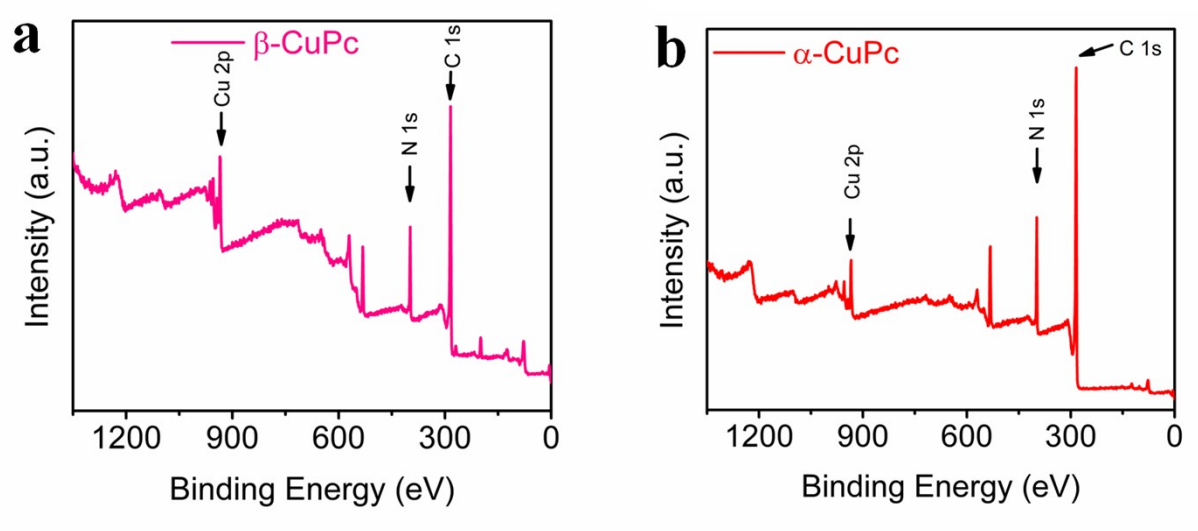

Fig. S2 (a)-(b) XPS survey scan of β-CuPc and α-CuPc respectively

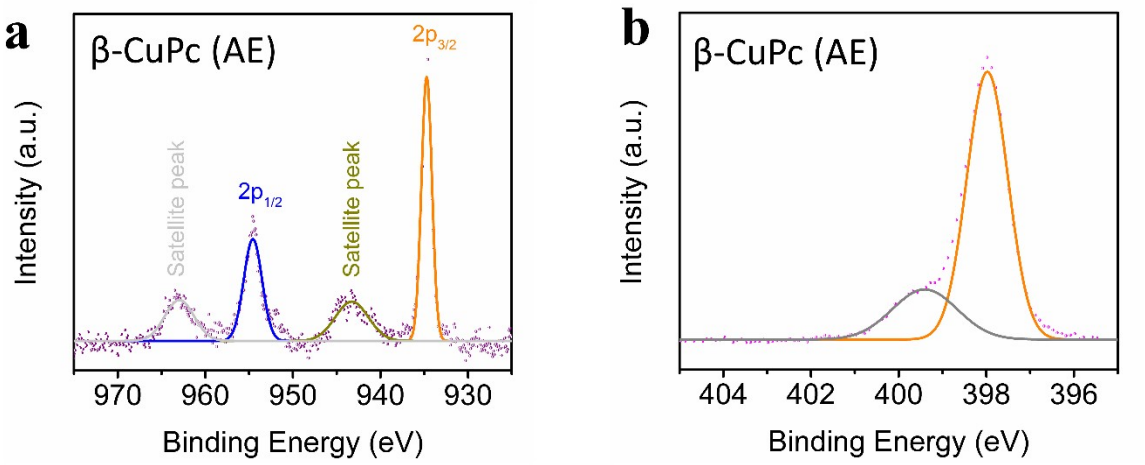

Fig. S3 (a)-(b) High resolution XPS spectra of Cu 2p and N1s of β-CuPc after electrocatalytic reaction respectively.

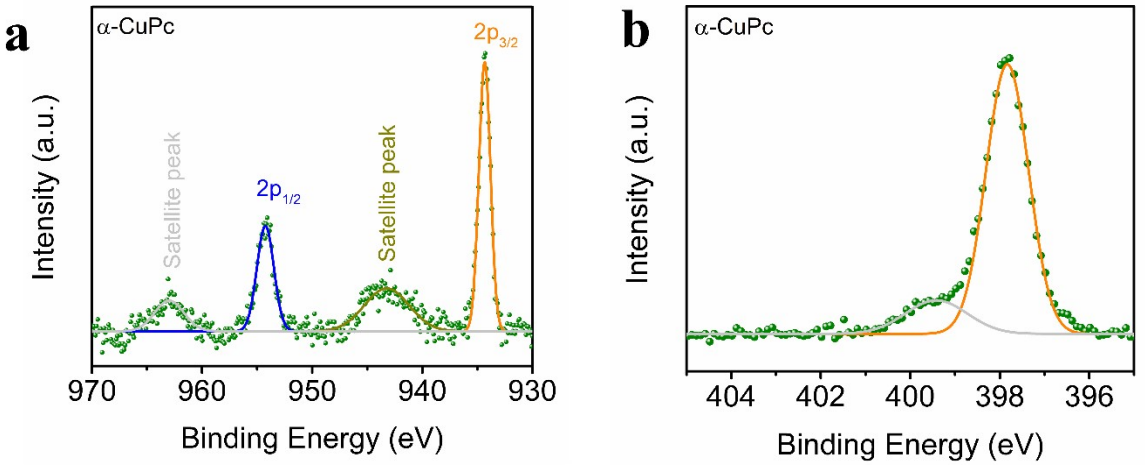

Fig. S4 (a)-(b) High resolution XPS spectra of Cu 2p and N1s of α-CuPc respectively.

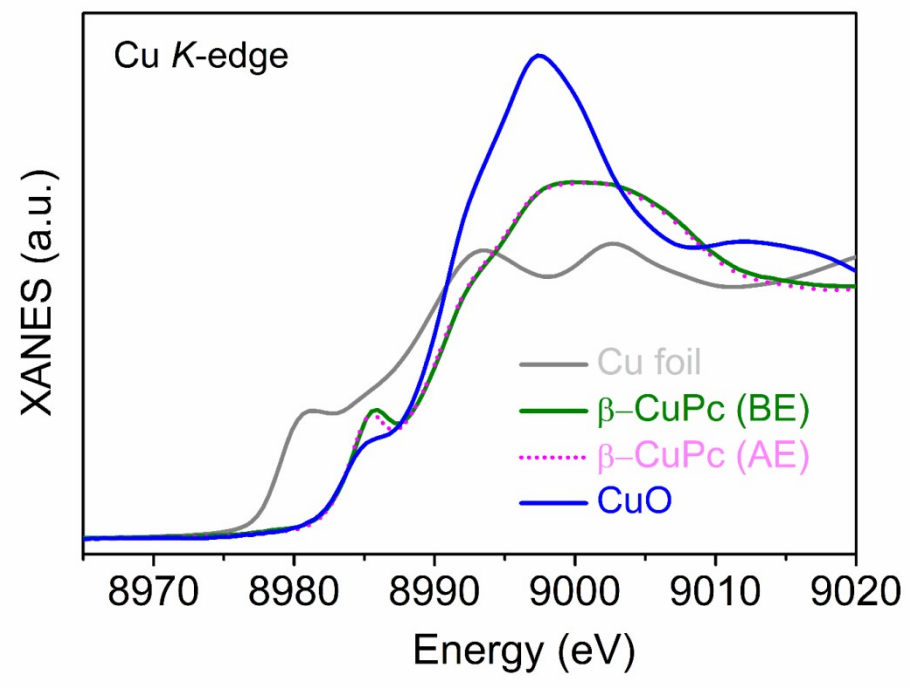

Fig. S5 XANES spectra of CuO, Cu foil, β-CuPc before and after electrocatalysis.

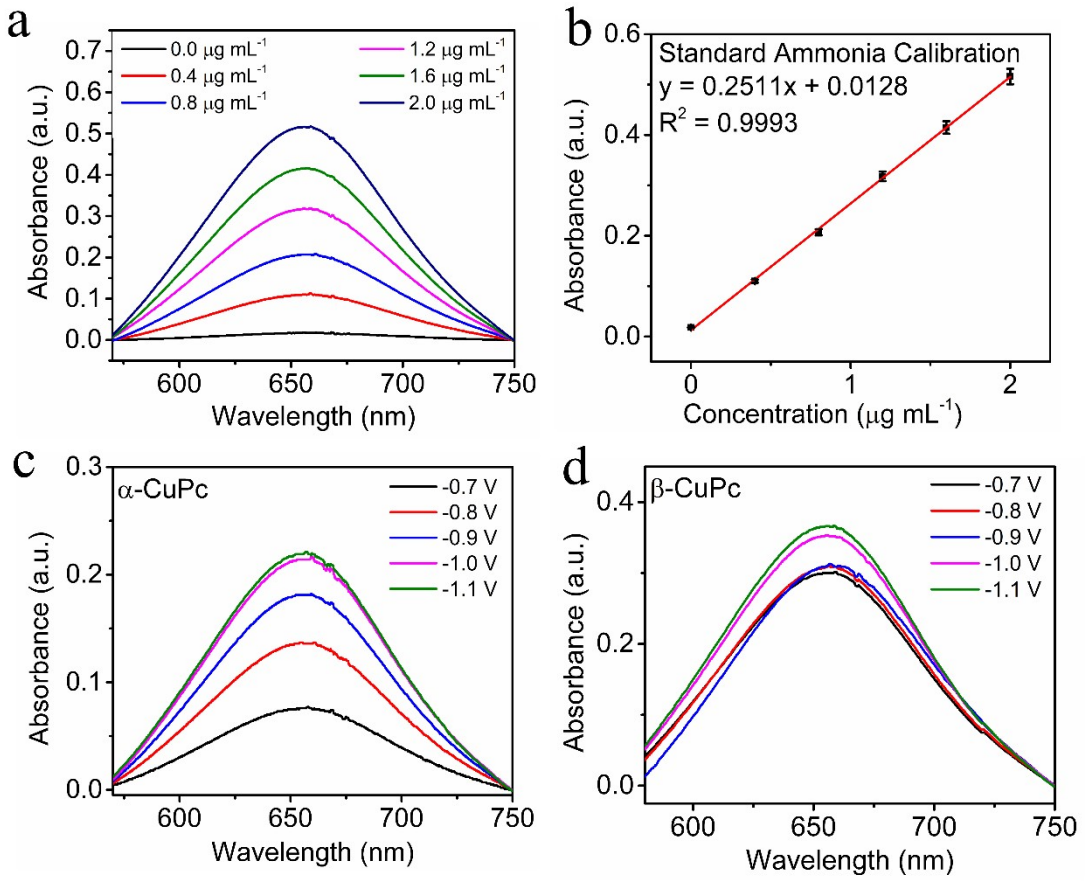

Fig. S6 (a) Spectrum of UV-vis absorption of different standard ammonia concentration series. (b) Calibration curve of standard ammonia from UV-vis spectroscopy solution used for unknown ammonia concentration determination (c) & (d) Spectrum of UV-vis absorption of ammonia electrocatalytically synthesised by α-CuPc & β-CuPc respectively after dilution.

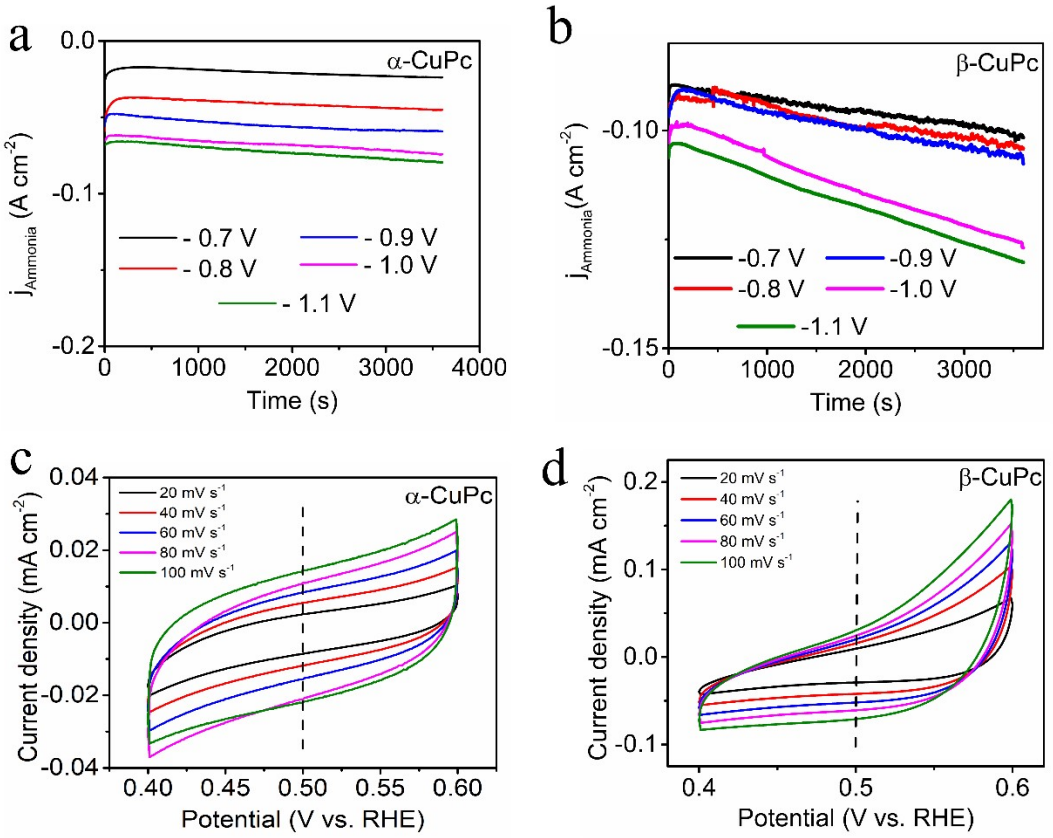

Fig. S7 (a) & (b) Chronoamperometric curves at different potential for 1h electrocatalytic nitrate reduction experiment of α-CuPc & β-CuPc respectively. (c-d) The cyclic Voltammetry (CV) profiles at the different sweep rates of α-CuPc & β-CuPc respectively.

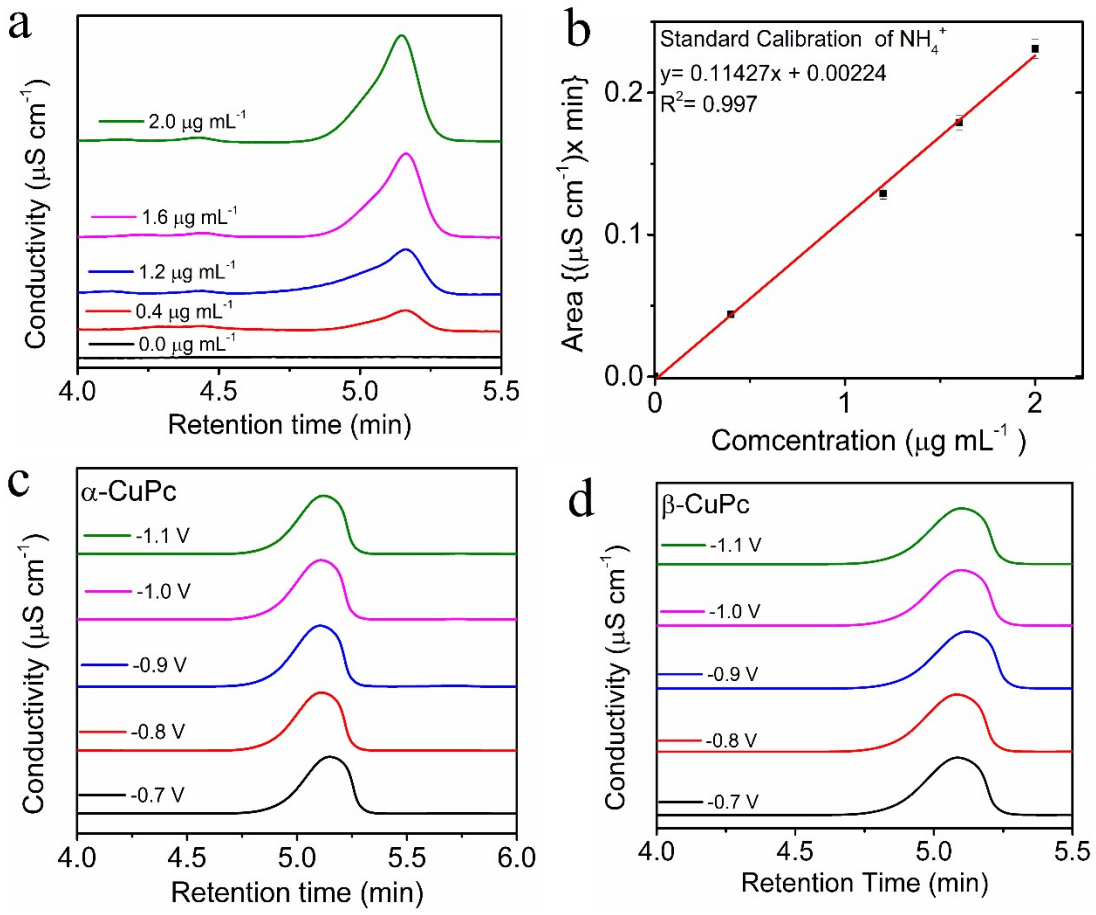

Fig. S8 (a) Conductivity vs retention time curve of different standard ammonia concentration series from ion chromatography. (b) Calibration curve from IC of standard ammonia solution used for unknown ammonia concentration determination (c) & (d) Conductivity vs retention time curve of ammonia electrochemically synthesised by α-CuPc & β-CuPc respectively after dilution from IC.

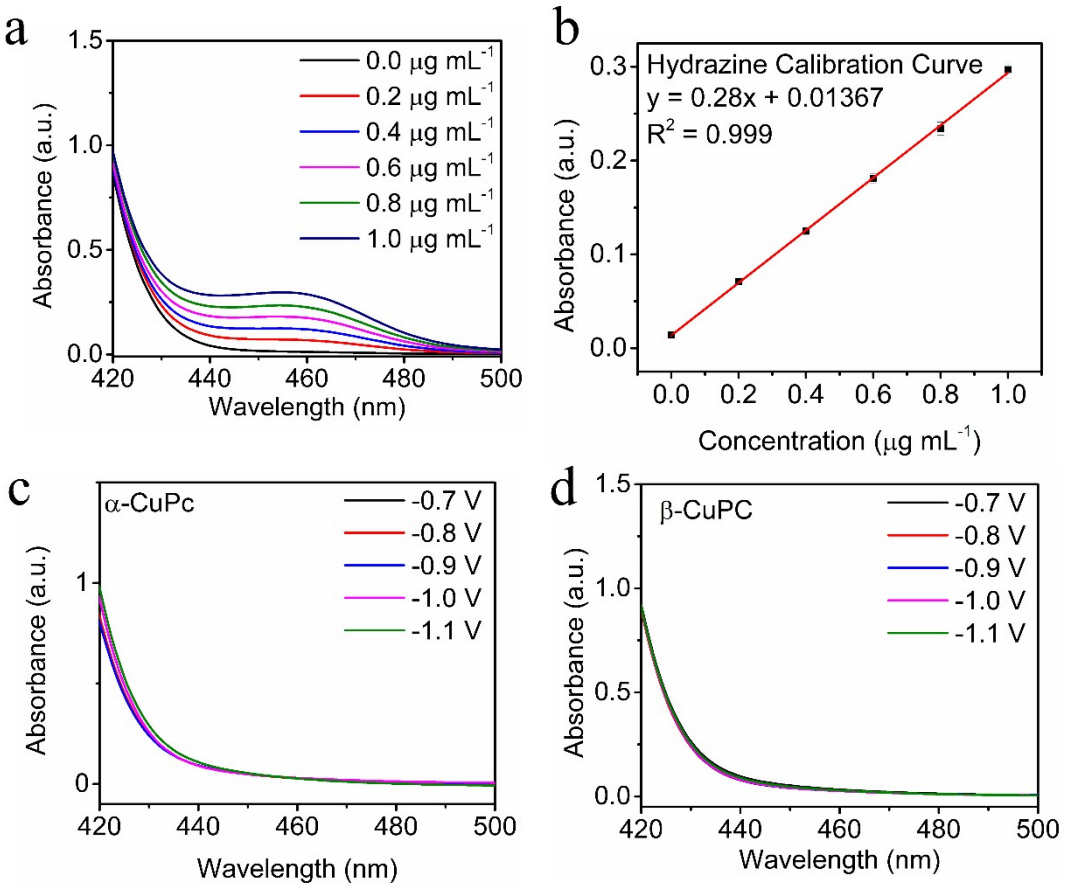

Fig. S9 (a) Spectrum of UV-vis absorption of different standard hydrazine concentration series. (b) Calibration curve of standard hydrazine from UV-vis spectroscopy solution used for unknown hydrazine concentration determination (c) & (d) Spectrum of UV-vis absorption of hydrazine electrocatalytically synthesised by α-CuPc & β-CuPc respectively.

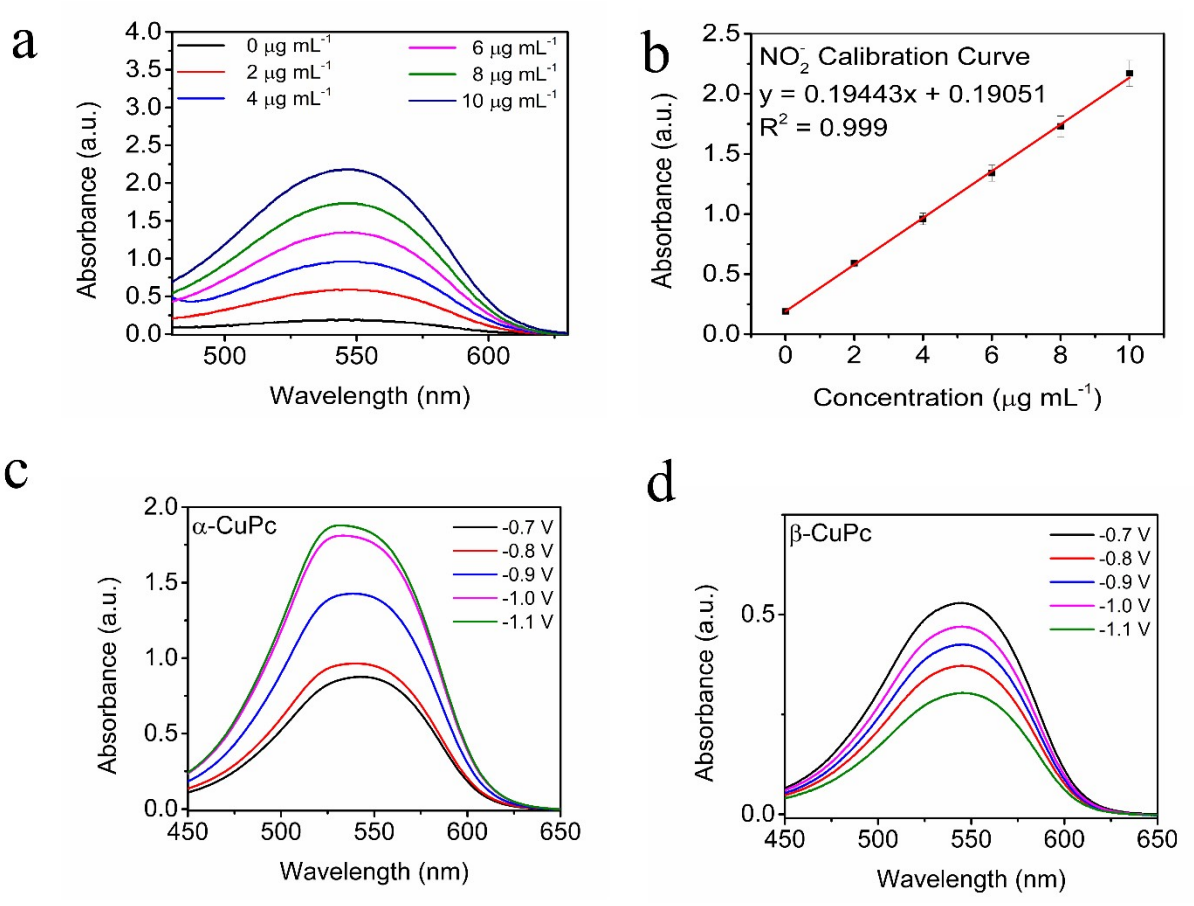

Fig. S10 (a) Spectrum of UV-vis absorption of different standard NO_2^- concentration series. (b) Calibration curve of standard NO_2^- from UV-vis spectroscopy solution used for unknown hydrazine concentration determination (c) & (d) UV-vis absorption spectra of NO_2^- electrocatalytically synthesised by α-CuPc & β-CuPc respectively.

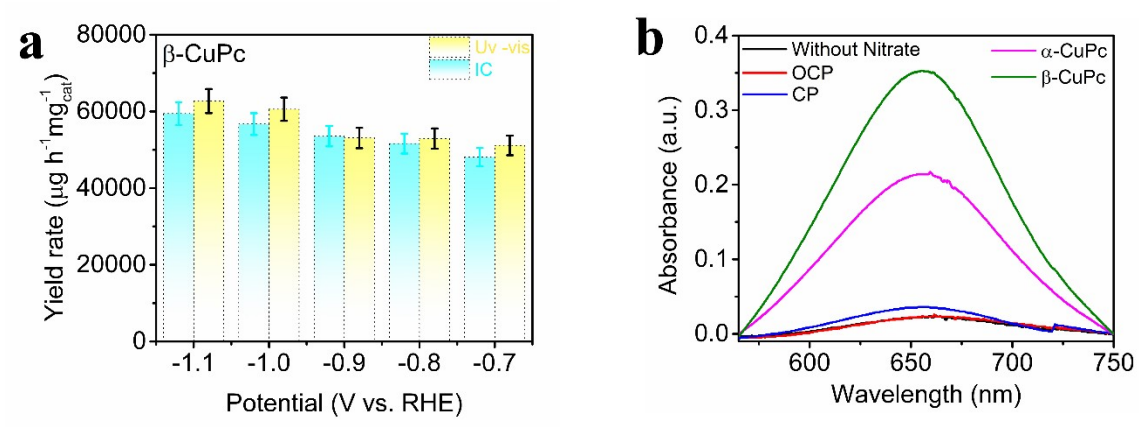

Fig. S11 (a) Comparison of the ammonia yield rate of β-CuPc via the indophenol method by UV-vis spectra and ion chromatography, **(b)** UV-vis spectra of indophenol reagent-stained electrolyte after electrocatalysis by α-CuPc (dil.), β-CuPc (dil.), and carbon paper at −1.1 V vs. RHE in the presence of 0.25 M $NaNO_3$ also at open-circuit potential and without nitrate solution using β-CuPc.

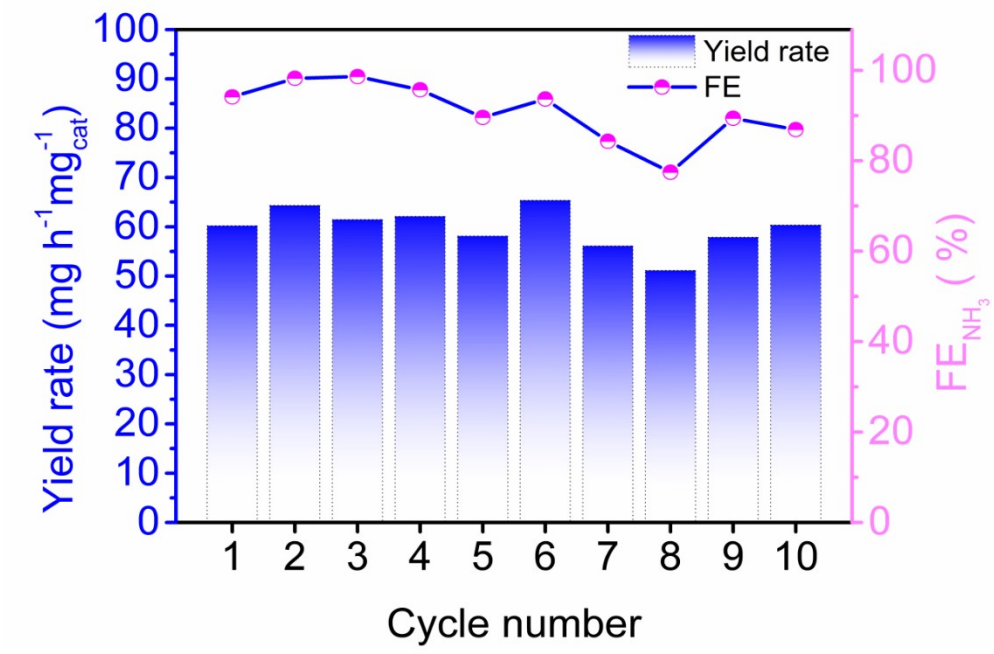

Fig. S12 Yield rate and Faradaic efficiency of β-CuPc up to 10 cycles of 5 hours each at -1.1 V vs. RHE.

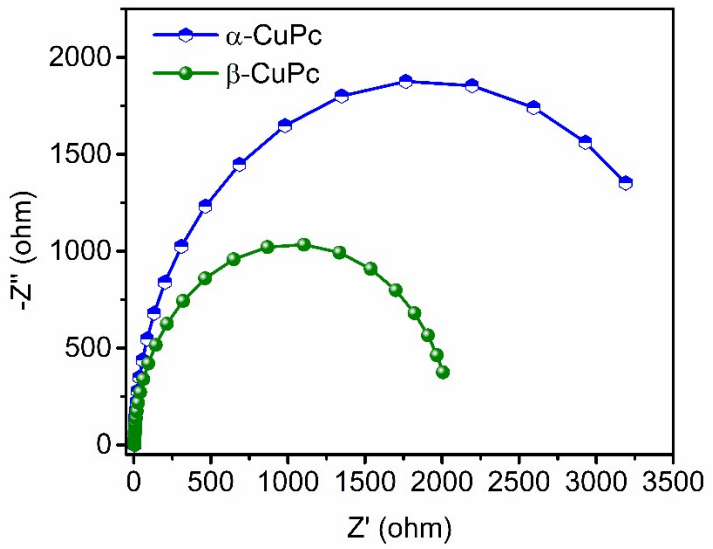

Fig. S13 EIS plot of α-CuPc and β-CuPc

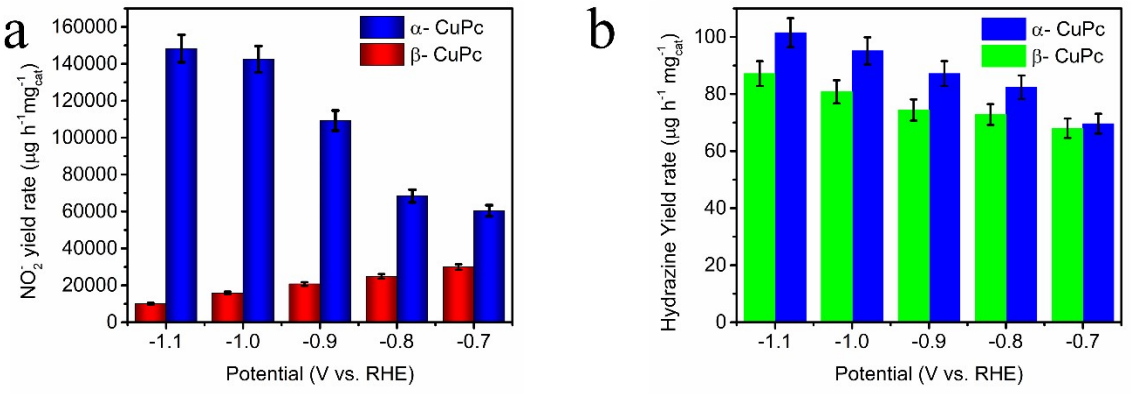

Fig. S14 (a) Nitrite and (b) Hydrazine yield rate for α- CuPc and β-CuPc

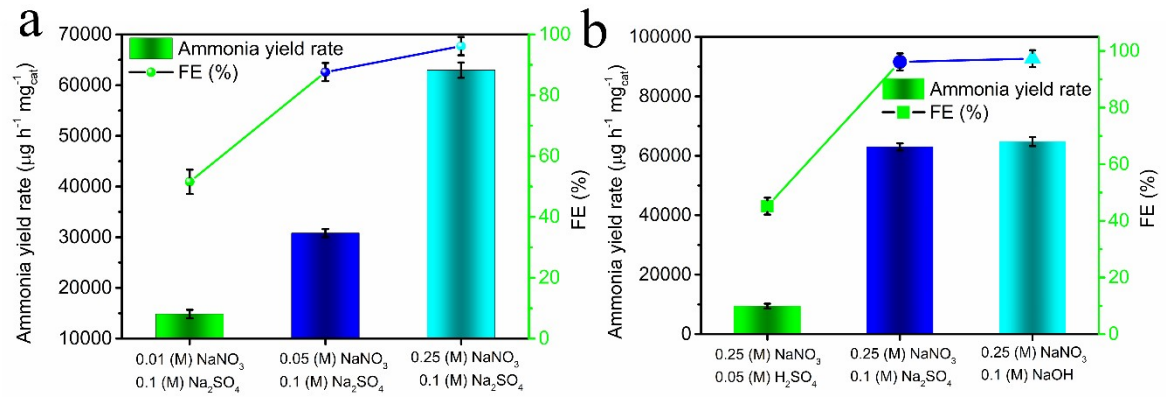

Fig. S15 (a) Ammonia yield rate and FE at different concentration of nitrate at -1.1 V vs. RHE, (b) Ammonia yield rate and FE at different pH at -1.1 V vs. RHE.

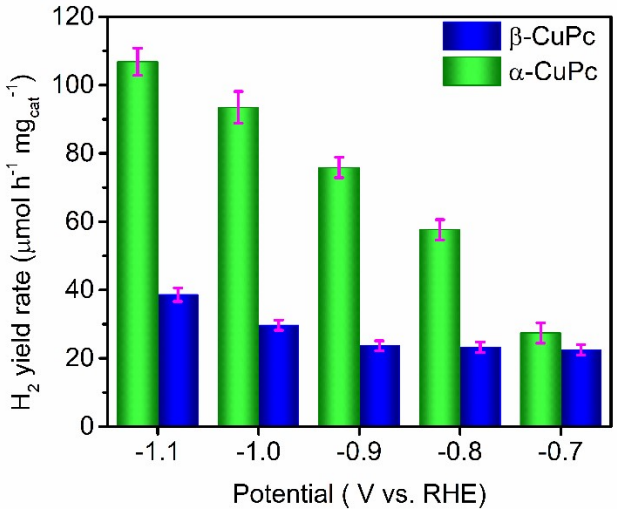

Fig. S16 Hydrogen evolution rate at different potential for α- CuPc and β-CuPc.

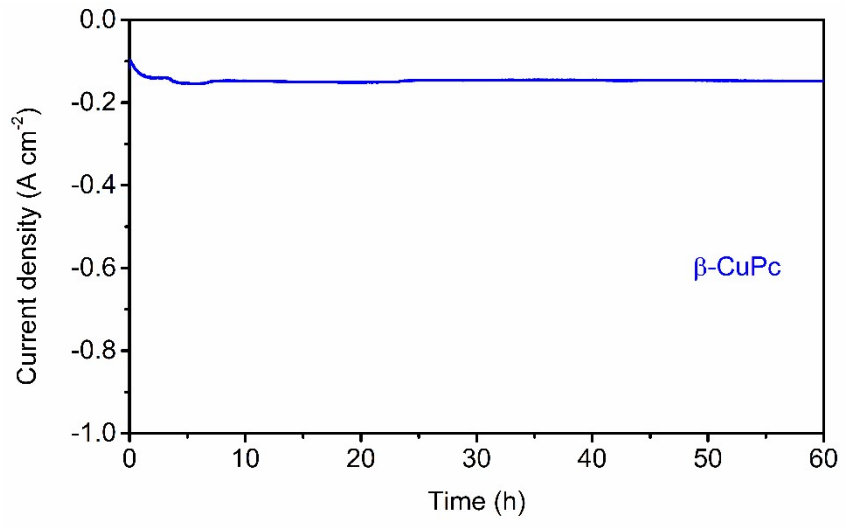

Fig. S17 Continuous long term (60 hours) stability of β-CuPc at -1.1 V vs. RHE.

Table-S1. Best fit data of EXAFS fitting of β-CuPc at Cu *K*-edge.

		β-CuPc
Cu-N	CN (4)	4±0.1
	R (Å) (1.95)	1.98±0.1
	σ^2	0.003±0.001
Cu-C	CN (8)	8±0.1
	R (Å) (2.99)	3.20±0.01
	σ^2	0.003±0.001

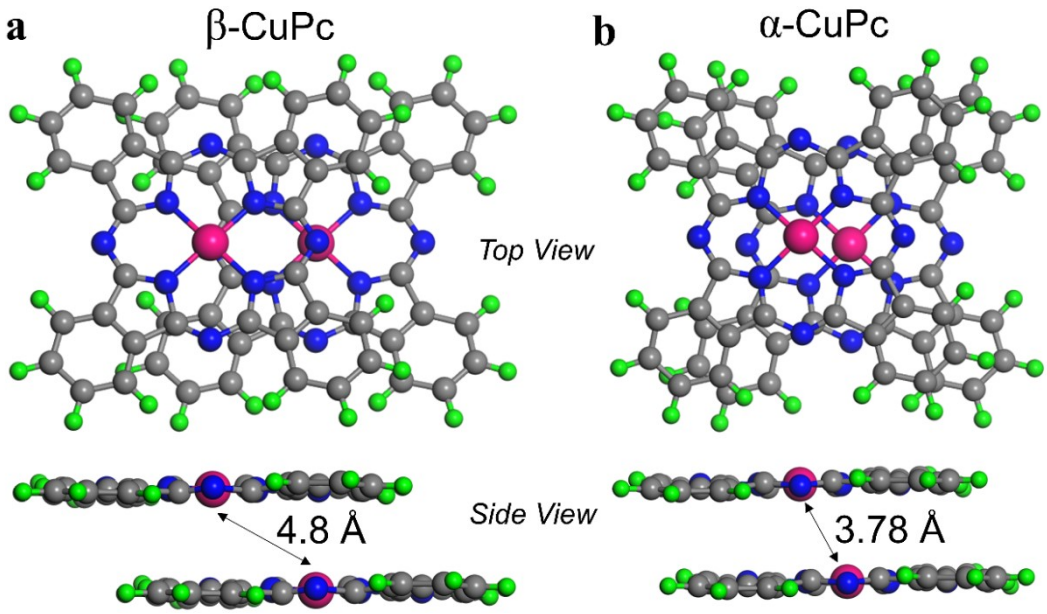

Fig. S18 Model structures of (a) β-CuPc (b) α-CuPc. The Cu, N, C, H atoms are denoted with pink, blue, gray and green color sphere respectively.

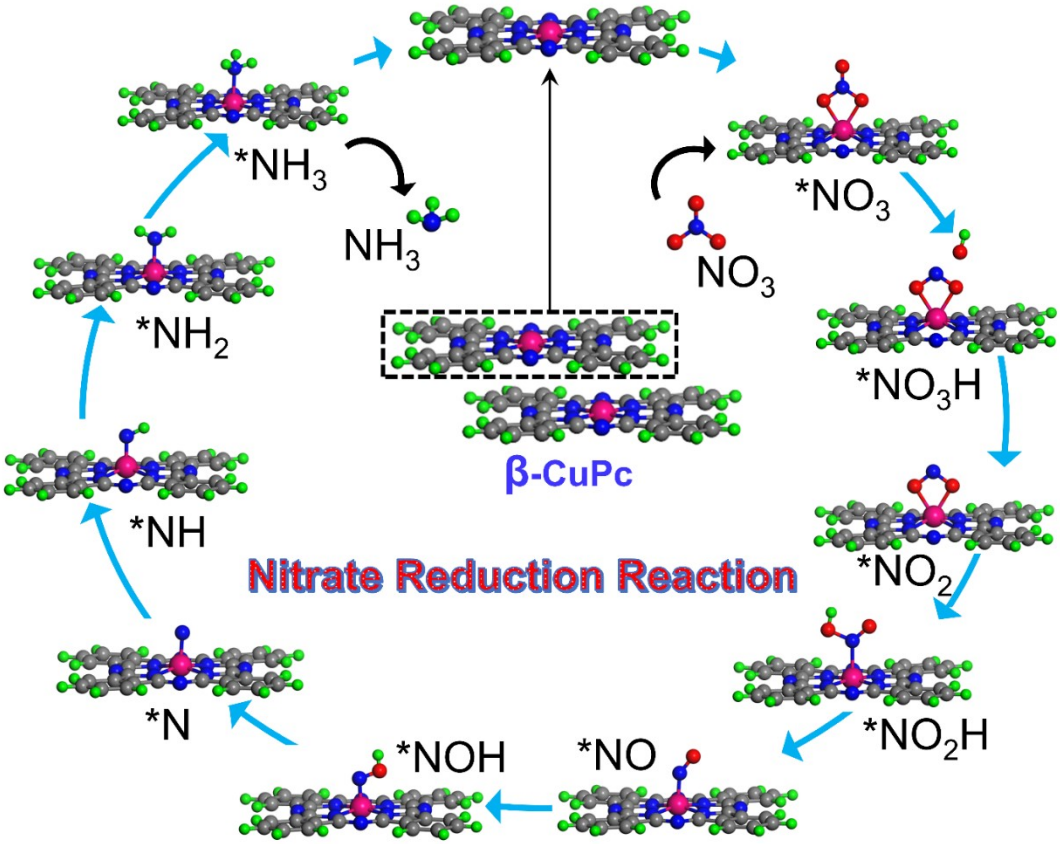

Fig. S19 The several stages of the nitrate reduction reaction (NO_3RR) are demonstrated on the Cu site of β-CuPc system (the symbol * denotes adsorption)

Table-S2. The DFT energy, ZPE, TS and gibbs free energy values for the free molecules and each intermediate adsorbed on β-CuPc. * Denotes for adsorbed case.

Species	E	ZPE	TS	G=E+ZPE-TS
NO_3	-23.32	0.33	0.75	-23.74
NH_3	-19.41	0.92	0.58	-19.07
H_2O	-14.33	0.56	0.67	-14.44
***NO_3**	-864.32	0.39	0.24	-864.17
***NO_3H**	-868.89	0.58	0.43	-868.74
***NO_2**	-858.69	0.25	0.22	-858.65
***NO_2H**	-863.05	0.57	0.27	-862.75
***NO**	-851.93	0.18	0.14	-851.89
***NOH**	-855.03	0.35	0.15	-854.82
***N**	-843.83	0.06	0.06	-843.83
***NH**	-848.61	0.32	0.10	-848.39
***NH_2**	-854.14	0.67	0.07	-853.53
***NH_3**	-859.74	1.02	0.15	-858.87

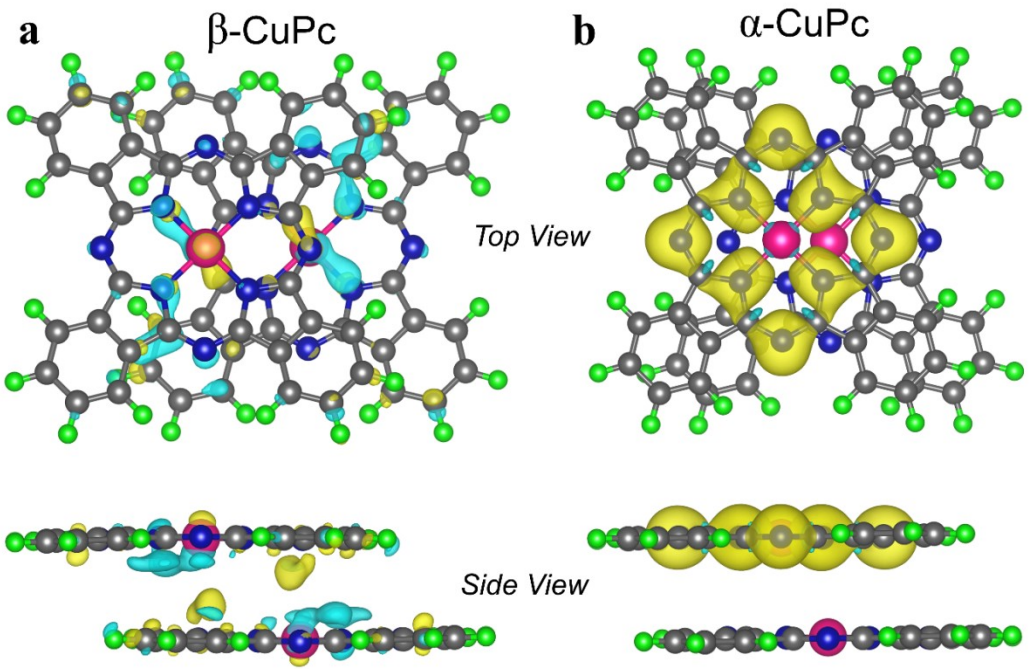

Fig. S20 The charge density difference analysis for (a) β-CuPc and (b) α-CuPc. The yellow and blue color region indicates charge accumulation and depletion respectively. (Isosurface value = 0.001 e/Å^3).

Table S3: Comparison of the NO_3RR activity for CuPc with others Cu based electrocatalysts in aqueous solution at ambient conditions

Catalyst	**Electrolyte**	**Yield rate**	**Faradaic efficiency**	**Reference**
CuPd-MOF	0.5 M K_2SO_4 + 50 mg L^{-1} KNO_3-N	1510.3 μg h^{-1} $mg^{-1}_{cat.}$	84.04 %	Applied Catalysis B: Environmental, 2022, 318, 121805
Zn−CuO NAs	0.1 M Na_2SO_4 + 0.01 M $NaNO_3$	945.1 μg h^{-1} cm^{-2}	95.6%	ACS Appl. Mater. Interfaces 2023, 15, 5172−5179
PTCDA-Metal catalyst	0.1 M PBS + 500 ppm	436 ± 85 μg h^{-1} cm^{-2}	85.90%	Nat. Energy 2020, 58, 5 (8),

	$NaNO_3$ + 0.001 M $CuSO_4$			605–613
CuO NWAs	0.5 M Na_2SO_4 + 200 ppm $NaNO_3$	0.2449 mmol h^{-1} cm^{-2}	95.80%	Angew. Chemie Int. Ed. 2020, 59 (13), 5350–5354
Cu-N-C-800	[initial NO_3-N] = 50 mg L−1; [Na_2SO_4] = 50 × 10−3 m	Conversion yield 97.3%	Current efficiency 19.5%	Small, 2020, 16 (49), 2004526
Cu(100) facets	1 M KOH + 5 mM KNO_3	---	87%	ACS Energy Lett. 2023, 8, 3658−3665
Cu-SnS_{2-x} nanoflowers	0.1 M KOH + 0.1 M KNO_3	0.63 mmol h^{-1} mg_{cat}^{-1}	93.8%	J. Mater. Chem. A, 2023, 11, 2014-2022
Cu/CuO_x/CF	0.5 M K_2SO_4 + 200 mg L^{-1} NO_3^--N	0.23 mmol h^{-1} cm^{-2}	93.58%	ACS Appl. Mater. Interfaces 2022, 14, 34761−34769
Cu-Pt nanointerfaces	0.1 mol L^{-1} Na_2SO_4 + 10 mmol $L^{-1}$$NaNO_3$	194.4 mg NH_3-N L^{-1} g_{cat}^{-1}	22%	Applied Catalysis B: Environmental, 2022, 302, 120844
Cu nanowires	0.1 M Na_2SO_4 + 0.1 M KNO_3	1.27 mmol h^{-1} cm^{-2}	93%	Angew. Chem. Int. Ed. 2022, 61, e202202556
Cu@CuHHTP	0.5 M Na_2SO_4 + 500 ppm NO_3^-	1.84 mg h^{-1} cm^{-2}	67.55%	ACS Appl. Mater. Interfaces 2022, 14, 32176−32182
Cu-N-C	0.1 M KOH + 0.1 M KNO_3	4.5 mg cm^{-2} h^{-1}	84.7%	J. Am. Chem. Soc. 2022, 144, 12062−12071

Ru-dispersed Cu nanowire	1 M KOH with 2,000 ppm NO_3^-	76,500 μg h^{-1} cm^{-2}	93%	Nat. Nanotechnol. 2022, 17 (7), 759–767
CNTs@mesoC @CuPd	0.1 m Na_2SO_4 + 100 mg L^{-1} NO_3^-	30 000 mg_{-N} g^{-1}	63.5%	Adv. Mater. 2023, 35 (2), 2207522
α-CuPc	**0.1 M Na_2SO_4 + 0.25 M $NaNO_3$**	**36,889 μg h^{-1} mg_{cat}^{-1}**	**61%**	**This work**
β-CuPc	**0.1 M Na_2SO_4 + 0.25 M $NaNO_3$**	**62,703 μg h^{-1} mg_{cat}^{-1}**	**96%**	**This work**

References

1 G. W. Watt and J. D. Chrisp, *Anal Chem*, 1952, **24**, 2006–2008.

2 G. Kresse and D. Joubert, *Phys Rev B*, 1999, **59**, 1758.

3 J. P. Perdew, K. Burke and M. Ernzerhof, *Phys Rev Lett*, 1996, **77**, 3865.

4 P. E. Blöchl, *Phys Rev B*, 1994, **50**, 17953.

5 S. Sinthika, U. V. Waghmare and R. Thapa, *Small*, 2018, **14**, 1703609.